Nonequilibrium-molecular-dynamics investigation of the presmectic behavior of the viscosities of a Gay-Berne nematic liquid crystal

Loris Bennett and Siegfried Hess
Institut für Theoretische Physik, Technische Universität Berlin, Berlin, Germany
(Received 31 March 1999)

Using the method of nonequilibrium molecular dynamics, the behavior of the Mięsowicz, Helfrich, and Leslie viscosities as functions of temperature and density are investigated. In particular, attention is focused on the region immediately preceding the nematic-smectic phase transition. The Mięsowicz viscosity η_1 for the orientation parallel to the direction of flow and the Helfrich viscosity η_{12} are both found to increase rapidly as the phase transition is approached. In most of the cases investigated, a critical exponent $\nu=\frac{1}{3}$ is found. Values closer to $\nu=\frac{1}{4}$ are also found, but in these cases, the errors are sufficiently large for $\nu=\frac{1}{3}$ to be possible. No nonregular behavior of the viscosity coefficients η_2, η_3, γ_1, and γ_2 in the presmectic region was detected. [S1063-651X(99)01710-9]

PACS number(s): 61.30.−v, 61.20.Ja, 62.10.+s, 66.20.+d

I. INTRODUCTION

For a nematic liquid crystal, the viscosity is a function of the average orientation of the molecules with respect to the flow velocity and its gradient. The shear viscosity is characterized by four quantities: the Mięsowicz viscosities η_i $(i=1,2,3)$ [1], and the Helfrich viscosity η_{12} [2]. Two further quantities of interest, the Leslie viscosities γ_1 and γ_2 [3], arise due to the torque acting on the molecules. These coefficients depend not only on the temperature (or density), but also on the proximity of the system to a phase boundary. In this work, attention will be focused on presmectic effects.

Although the effect of temperature on the viscosity of a freely flowing liquid crystal was first measured [4] at the end of the last century, measurements of the temperature dependence of the coefficients η_i and γ_1 close to the nematic-smectic transition have only been available since the mid-1970s [5–12]. Divergent behavior for η_1 and γ_1 is found for several substances, but it has often proved difficult to determine critical exponents.

Viscous flow in nematic fluids has also been investigated using the methods of *equilibrium molecular dynamics* (MD) and *nonequilibrium molecular dynamics* (NEMD) at single state points [13,14]. For perfectly oriented particles interacting via a soft-sphere potential with an additional anisotropic term of P_2 symmetry a reversal of the inequality $\eta_1<\eta_2$ for temperatures just above the nematic-smectic transition has been found [15].

The Mięsowicz coefficients of the standard Gay-Berne system have been obtained as a function of temperature for one density using MD and the Green-Kubo relations [16]. Although a sharp rise in η_1 was observed just above T_{na}, the critical exponent was not determined. Results have also been obtained in the case of a soft-sphere potential plus a dipole-dipole interaction [17]. Here, a reordering of the Mięsowicz coefficients η_1 and η_2 is found as the relative strength of the anisotropic term is increased. Simulations using the Gay-Berne potential and a director-based coordinate system [18] show good agreement with the results of [16] for a single state point as far as η_2 and η_3 are concerned. However, a considerable discrepancy exists for both η_1 and γ_1.

Thus, up to now, there has been little simulation data available on the presmectic behavior of the Mięsowicz coefficients, with most of the work mentioned focusing on a single state point, rather than a range of temperatures or densities. This is not surprising considering the demands made on computational resources by even fairly simple models for anisotropic fluids. However, it was felt that taking a more detailed look at the way the presence of the nematic-smectic transition affects rheological properties would be a worthwhile undertaking.

The work presented here is structured as follows: After this Introduction, the theoretical description of viscosity for an anisotropic fluid is summarized. In the following section, the effect of temperature and density variation as well as that of an external field on the various coefficients of viscosity are discussed. In Sec. IV, details of the simulation method are given. Section V comprises the results and their interpretation. The conclusions are presented in the final section.

II. VISCOSITY COEFFICIENTS OF A NEMATIC LIQUID CRYSTAL

In order to specify the various coefficients of viscosity, an ansatz must be made for the friction pressure tensor. If ρ is the mass density of a fluid, $\boldsymbol{v}$ the flow velocity, and Cartesian coordinates are used, then the equation for the balance of linear momentum may be written as

$$\rho\frac{d}{dt}v_\mu+\boldsymbol{\nabla}_\nu P^{\mathrm{eq}}_{\nu\mu}+\boldsymbol{\nabla}_\nu p_{\nu\mu}=0, \tag{1}$$

where the substantial time derivative is given by $d/dt=\partial/\partial t+v_\lambda\boldsymbol{\nabla}_\lambda$. The total pressure tensor $P_{\nu\mu}$ has been separated into its equilibrium part $P^{\mathrm{eq}}_{\nu\mu}$ and the friction pressure tensor $p_{\nu\mu}$.

For an isotropic fluid, the friction pressure tensor depends only on the spatial derivatives of the velocity field and the corresponding coefficients of viscosity. However, in the case of a nematic liquid crystal, the translational motion is coupled with the rotational motion. The orientation of the nematic may be described by a so-called *director field* $\boldsymbol{n}(\boldsymbol{r},t)$.

For the friction pressure tensor $p_{\mu\nu}$ an ansatz [19] is made which takes into account the nematic symmetry and assumes linearity in the velocity gradient and the corotational time derivative of the director $\boldsymbol{N}$:

$$\begin{aligned}-p_{\nu\mu}=&\alpha_1 n_\nu n_\mu n_\lambda n_\kappa \Gamma_{\lambda\kappa}+\alpha_2 n_\nu N_\mu+\alpha_3 n_\mu N_\nu+\alpha_4\Gamma_{\nu\mu}\\&+\alpha_5 n_\nu n_\lambda\Gamma_{\lambda\mu}+\alpha_6 n_\mu n_\lambda\Gamma_{\lambda\nu}+\zeta_1 n_\lambda n_\kappa\Gamma_{\lambda\kappa}\delta_{\mu\nu}\\&+\zeta_2 n_\nu n_\mu \nabla_\lambda v_\lambda+\zeta_3\nabla_\lambda v_\lambda\delta_{\mu\nu},\end{aligned}\tag{2}$$

where

$$N_\mu=\frac{d}{dt}n_\mu-\epsilon_{\mu\nu\lambda}\omega_\nu n_\lambda.\tag{3}$$

The gradient of the velocity $\nabla_\nu v_\mu$ has been decomposed into its isotropic, antisymmetric, and symmetric traceless parts:

$$\nabla_\nu v_\mu=\frac{1}{3}\nabla_\lambda v_\lambda\delta_{\mu\nu}+\epsilon_{\nu\mu\lambda}\omega_\lambda+\Gamma_{\nu\mu},\tag{4}$$

where ω_λ is the vorticity:

$$\omega_\lambda=\frac{1}{2}\epsilon_{\lambda\alpha\beta}\nabla_\alpha v_\beta,\tag{5}$$

and $\Gamma_{\nu\mu}$ the deformation rate tensor, which is the symmetric traceless part (denoted by $[\ ]_{\mathrm{ST}}$) of the velocity gradient tensor:

$$\Gamma_{\nu\mu}=[\nabla_\nu v_\mu]_{\mathrm{ST}}=\frac{1}{2}(\nabla_\nu v_\mu+\nabla_\mu v_\nu)-\frac{1}{3}\nabla_\lambda v_\lambda\delta_{\mu\nu}.\tag{6}$$

The coefficients $\alpha_1,\ldots,\alpha_6$, known as the Leslie coefficients, and the coefficients ζ_1, ζ_2, and ζ_3 all have the dimensions of a viscosity. Thus, once the velocity and director fields are known, the components of the friction pressure tensor may be calculated in terms of the α_i and ζ_i.

Decomposition of the friction pressure tensor yields

$$\begin{aligned}[p_{\nu\mu}]_{\mathrm{ST}}=&-2\eta\Gamma_{\nu\mu}-2\tilde{\eta}_1[n_\nu n_\lambda\Gamma_{\lambda\mu}]_{\mathrm{ST}}-2\tilde{\eta}_2[n_\nu N_\mu]_{\mathrm{ST}}\\&-2\tilde{\eta}_3[n_\nu n_\mu]_{\mathrm{ST}}n_\lambda n_\kappa\Gamma_{\lambda\kappa}-\zeta_2[n_\nu n_\mu]_{\mathrm{ST}}\nabla_\lambda v_\lambda,\end{aligned}\tag{7}$$

$$p^a_{\nu\mu}=\gamma_1(n_\nu N_\mu)^a+\gamma_2(n_\nu n_\lambda\Gamma_{\lambda\mu})^a,\tag{8}$$

$$\frac{1}{3}p_{\lambda\lambda}=-\eta_V\nabla_\lambda v_\lambda-\kappa n_\lambda n_\kappa\Gamma_{\lambda\kappa}.\tag{9}$$

The antisymmetric part of a tensor $T_{\nu\mu}$ is given by

$$T^a_{\nu\mu}=\frac{1}{2}(T_{\nu\mu}-T_{\mu\nu}).\tag{10}$$

The viscosity coefficients appearing in Eqs. (7)–(8) are related to those of Eq. (2) via

$$\eta=\frac{1}{2}\left[\alpha_4+\frac{1}{3}(\alpha_5+\alpha_6)\right],\tag{11}$$

$$\tilde{\eta}_1=\frac{1}{2}(\alpha_5+\alpha_6),\tag{12}$$

$$\tilde{\eta}_2=\frac{1}{2}(\alpha_2+\alpha_3),\tag{13}$$

$$\tilde{\eta}_3=\frac{1}{2}\alpha_1,\tag{14}$$

$$\gamma_1=\alpha_3-\alpha_2,\tag{15}$$

$$\gamma_2=\alpha_6-\alpha_5,\tag{16}$$

$$\eta_V=\frac{1}{3}\zeta_2+\zeta_3,\tag{17}$$

$$\kappa=\zeta_1+\frac{1}{3}(\alpha_1+\alpha_5+\alpha_6).\tag{18}$$

The nine viscosity coefficients of Eq. (2) are reduced to seven due to two Onsager symmetry relations, which yield

$$2\tilde{\eta}_2=\gamma_2,\tag{19}$$

which is equivalent to

$$\alpha_2+\alpha_3=\alpha_6-\alpha_5,\tag{20}$$

and

$$\zeta_2=\kappa.\tag{21}$$

As mentioned already, the Mięsowicz coefficients of viscosity are defined for certain orientations of the molecules with respect to the applied shear:

$$-p_{yx}=\eta_i\frac{\partial v_x}{\partial y},\quad i=1,2,3,4.\tag{22}$$

For Couette flow, the velocity field is given by $\boldsymbol{v}=(\Gamma y,0,0)$, where Γ is the shear rate, and thus, $\partial v_x/\partial y=\Gamma$.

Hence, one obtains the following relationships between the Mięsowicz viscosities and the coefficients used in the ansatz Eq. (2):

$$\eta_1=\frac{1}{2}(\alpha_4+\alpha_6+\alpha_3),\tag{23}$$

$$\eta_2=\frac{1}{2}(\alpha_4+\alpha_5-\alpha_2),\tag{24}$$

$$\eta_3=\frac{1}{2}\alpha_4.\tag{25}$$

The shear viscosity is characterized by four coefficients for this geometry and so a further quantity is needed. The Helfrich viscosity, η_{12} [2], is defined as

$$\eta_{12}=4\eta_4-2(\eta_1+\eta_2),\tag{26}$$

where η_4 is the viscosity obtained for the orientation in the xy plane which makes an angle of 45° with respect to the direction of flow. This leads to

$$\eta_{12}=\alpha_1. \tag{27}$$

The Leslie viscosities, γ_1 and γ_2, are given by

$$\gamma_1=\frac{1}{\Gamma}(p^1_{xy}-p^1_{yx}+p^2_{xy}-p^2_{yx}) \tag{28}$$

and

$$\gamma_2=\frac{1}{\Gamma}(p^1_{xy}-p^1_{yx}-p^2_{xy}+p^2_{yx}), \tag{29}$$

where $p^i_{\mu\nu}$ is the (μ,ν) component of the friction pressure tensor for the orientation parallel to the i axis. Equation (19) implies

$$\gamma_2=\eta_1-\eta_2. \tag{30}$$

The Mięsowicz, Helfrich, and Leslie viscosities are all accessible to experiment. Thus, values extracted from simulations may be compared with experimentally obtained results. Furthermore, a theoretical prediction of the relative sizes of the η_i and γ_i based on a modified affine transform approach may be given in terms of the axis ratio of ellipsoidally symmetric particles [20]. Thus one obtains information about the α_i, but the ζ_i are not determined here.

III. TEMPERATURE AND DENSITY DEPENDENCE

Any quantification of changes in viscous behavior as a phase transition is approached requires a functional form for the dependency. According to the reaction-rate approach, the dependency of the viscosity on the temperature in isotropic liquids is given approximately by an expression of the Arrhenius type:

$$\eta=a\exp(E/k_BT), \tag{31}$$

where $E>0$ is an activation energy, k_B Boltzmann's constant, T the temperature, and a a constant [21]. In the nematic phase, there will be an additional dependence on orientational order. However, the dependence of the order parameter on temperature is weak compared to that in Eq. (31) [21].

A form for the variation of the viscosity as a function of density may be given in terms of the *free volume*, $V_f=V-V_m$, where V is the specific volume of the fluid ($V=1/\rho$) and V_m is the specific volume of the molecules [22]. One then has $\eta(V)=a\exp[\epsilon V_m/(V-V_m)]$, or, in terms of the density,

$$\eta(\rho)=a\exp\left(\epsilon\frac{V_m}{1/\rho-V_m}\right), \tag{32}$$

where a is the low density limit of viscosity [in general not the same as a of Eq. (31)], and ϵ a dimensionless parameter. Within the framework of a computer simulation, V_m may be determined approximately from the form of the intermolecular potential used and here was taken to be the volume of an ellipsoid of rotation with short and long axes of length 0.5 and 1.5, respectively, the unit of length being the short molecular diameter.

For an anisotropic fluid, the behavior is somewhat different, particularly in the vicinity of a phase transition. In the case of the nematic-smectic transition, there is expected to be a contribution to the viscosity which depends on the *coherence length* ξ of the smectic order, which is the distance over which the smectic order parameter persists in the nematic phase.

According to the mean-field approach [23], the dependence of ξ on temperature is given by

$$\xi\sim(T-T_{na})^{-1/2}. \tag{33}$$

However, assuming the validity of de Gennes's analogy between the nematic-smectic phase change and the normal-superfluid transition in liquid helium [24], one infers

$$\xi\sim(T-T_{na})^{-2/3}. \tag{34}$$

The relationship between the coherence length and the Mięsowicz viscosities is given by Jähnig and Brochard [25]. They find the expressions

$$\gamma_1^{\rm crit}\sim\xi^{1/2}, \tag{35}$$

$$\alpha_1^{\rm crit}\sim\gamma_1^{\rm crit}, \tag{36}$$

$$\alpha_2^{\rm crit}=\alpha_4^{\rm crit}=\alpha_5^{\rm crit}=0, \tag{37}$$

$$\alpha_3^{\rm crit}=\gamma_2^{\rm crit}=\gamma_1^{\rm crit}, \tag{38}$$

where the superscript ''crit'' indicates that contribution of the quantity due to thermal fluctuation of the smectic order parameter above T_{na}. Thus, from the expressions for the Mięsowicz viscosities, and for the Helfrich viscosity, one obtains

$$\eta_1^{\rm crit}\sim\eta_{12}^{\rm crit}\sim\xi^{1/2}, \tag{39}$$

$$\eta_2^{\rm crit}=\eta_3^{\rm crit}=0. \tag{40}$$

Thus, η_1, η_{12}, γ_1, and γ_2 as functions of temperature are all expected to diverge as the nematic-smectic transition is approached. The total viscosity, including the Arrhenius term, has the form

$$\eta(T)=a\exp(\epsilon/T)+b(T-T_{na})^{-\nu}, \tag{41}$$

where ν is $\frac{1}{4}$ for the mean-field approach and $\frac{1}{3}$ according to the helium analogy.

It must be borne in mind that increasing the temperature will lead to an increase in the effective volume of the particles due to the increased rotational fluctuation. At constant *pressure*, the total volume can change and thus compensate for the effect on the free volume. In this case the Arrhenius law can be expected to apply and the viscosity will fall with increasing temperature. However, at constant *volume*, no such compensation can take place, and thus although the increase in translational kinetic energy will still act to reduce the viscosity, the accompanying increase in the rotational

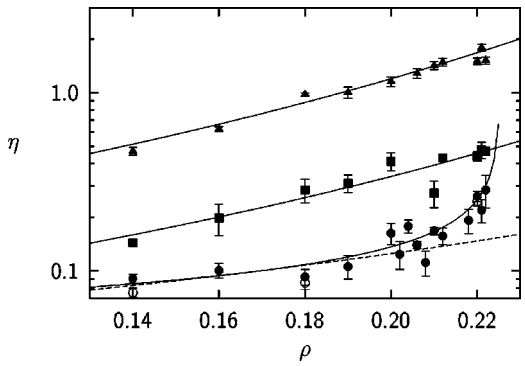

FIG. 1. The Mięsowicz viscosities as functions of density for $T=0.95$ with $B=0.90$, $N=500$: η_1 (●), η_2 (▲), and η_3 (■) with fits (regular component ——, divergent component − − −), and $N=1372$: η_1 (○).

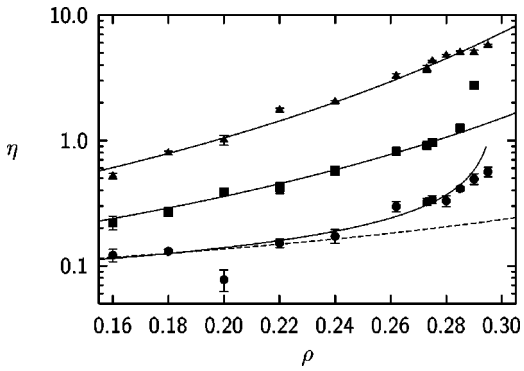

FIG. 2. η_1 (●), η_2 (▲), and η_3 (■) as functions of density for $T=0.95$ with $B=0.35$, together with fits (regular component ——, divergent component − − −) .

kinetic energy will have the opposite effect. Therefore, the behavior is more complicated than in the case of constant pressure. In particular, even a fall in viscosity with decreasing temperature is possible.

Expressions corresponding to those for the temperature may be obtained for the density dependence of the critical components of the viscosities. A transition temperature T^* at which a phase transition in a liquid crystal occurs will be a function of the density. Thus, assuming that T^* is a linear function of ρ, one has

$$T^*(\rho)=T_0^*+T^{*\prime}(\rho-\rho_0), \tag{42}$$

where ρ_0 is a particular density and $T^{*\prime}$ the derivative of T^* with respect to ρ. For a certain temperature T, this then yields $1-T^*/T=1-[T_0^*+T^{*\prime}(\rho-\rho_0)]/T$. Therefore,

$$1-\frac{T^*}{T}\sim 1-\frac{\rho}{\rho^{\mathrm{ref}}},\quad \rho^{\mathrm{ref}}=\rho_0+\frac{T-T_0^*}{T^{*\prime}}. \tag{43}$$

Thus, Eq. (43) means that the critical exponent for the density dependency is the same as that for the temperature dependency. Together with Eq. (32), this leads to an expression for the viscosity as a function of density very similar to Eq. (41):

$$\eta(\rho)=a\exp\left(\epsilon\frac{V_m}{1/\rho-V_m}\right)+b(\rho_{na}-\rho)^{-\nu}. \tag{44}$$

Again, for simplicity, the same symbols for the parameters a, b, and ϵ as in Eq. (41) have been used, although in general they are obviously numerically different. As above, V_m is the specific volume of a molecule.

TABLE I. Fit parameters for the density dependence with $T=0.95$, $B=0.90$.

η_1, div.	$b=0.03\pm0.01$	$\nu=0.39\pm0.08$	$\rho_{na}=0.23\pm0.01$
η_1, reg.	$a=0.04\pm0.01$	$\epsilon=2.34\pm0.93$	
η_2, reg.	$a=0.13\pm0.02$	$\epsilon=4.80\pm0.30$	
η_3, reg.	$a=0.05\pm0.01$	$\epsilon=4.28\pm0.24$	

TABLE II. Fit parameters for the density dependence with $T=0.95$, $B=0.35$.

η_1, div.	$b=0.04\pm0.02$	$\nu=0.56\pm0.23$	$\rho_{na}=0.30\pm0.02$
η_1, reg.	$a=0.08\pm0.02$	$\epsilon=1.25\pm0.71$	
η_2, reg.	$a=0.14\pm0.02$	$\epsilon=4.46\pm0.21$	
η_3, reg.	$a=0.08\pm0.01$	$\epsilon=3.32\pm0.16$	

IV. SIMULATION METHOD

The simulations were performed using standard constant temperature and volume molecular-dynamics techniques. The Gay-Berne potential [26] was used with the parameters $\mu=2$, $\nu=1$, $\kappa=3$, and $\kappa'=5$ to model the intermolecular interaction, the phase diagram for these values being known [27]. The equations of translational and rotational motion were derived from the derivative of the potential with respect to the intermolecular displacement vector and the molecular orientation vector, respectively. The potential was truncated and shifted at a cutoff radius of $4\sigma_0$, where σ_0 is the width of the molecules. The equations were then solved via a Verlet velocity algorithm [28]. The mass and the moment of inertia were chosen to be equal to unity, with the time step being of length $0.0015(m\sigma_0^2/\epsilon_{LJ})$, where ϵ_{LJ} is the reference energy. Lees-Edwards periodic boundary conditions [29] were used to generate the shear. The temperature derived from the translational motion was held constant by means of a profile-unbiased Gaussian thermostat [30], which simply involves rescaling the peculiar velocities. The rotational motion was not explicitly thermostated, as the coupling to the translational motion was found to be strong enough to produce satisfactory equipartition of the total kinetic energy. Unless mentioned otherwise, 500 particles were used. However, a few simulations were carried out with $N=1372$, in order to check for possible finite-size effects.

Newtonian viscosities were obtained by evaluating the appropriate components of the pressure tensor for various values of the shear rate (typically 0.01, 0.02, 0.03, 0.04, 0.05 in reduced units) and extrapolating to zero shear rate under the assumption that there is no shear-rate dependency in this regime.

The orientation of the particles must be fixed in a certain direction in order to allow the calculation of the Mięsowicz coefficients. This can either be done by means of a constraint

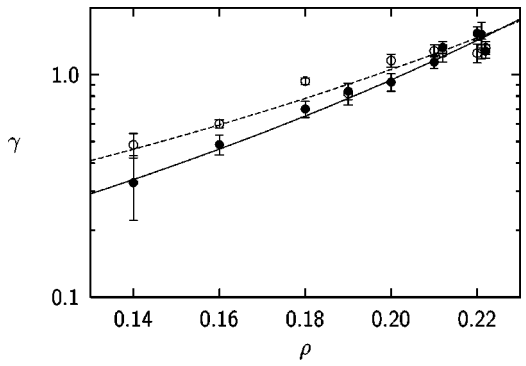

FIG. 3. γ_1 (●) with fit (——) and $-\gamma_2$ (○) with fit (− − −) as functions of density for $T=0.95$ with $B=0.90$.

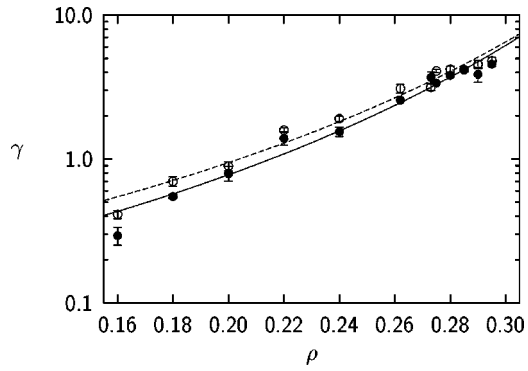

FIG. 4. γ_1 (●) with fit (——) and $-\gamma_2$ (○) with fit (− − −) as functions of density for $T=0.95$ with $B=0.35$.

algorithm [31], or via an additional potential term which makes the alignment of the molecules with the field energetically more favorable. Here, the latter approach was taken and the simulation box chosen to be twice as long in the direction parallel to the field as in the perpendicular directions. The effect on the viscosity of the variation of the field strength in the range before orientational saturation sets in has also been studied [32].

The energy density f_M, which arises due to the coupling between a molecule and an applied magnetic field $\boldsymbol{B}$, is taken to be

$$f_M = -\frac{1}{2}\mu_0^{-1}\Delta\chi([\boldsymbol{uu}]_{\mathrm{ST}}:[\boldsymbol{BB}]_{\mathrm{ST}}), \tag{45}$$

where $\Delta\chi=\chi_\parallel-\chi_\perp$, $\chi_\parallel$ and $\chi_\perp$ being the susceptibility parallel and perpendicular to the director, respectively (cf. [33]). The orientation-dependent part reduces to $f_M = -\frac{1}{2}\mu_0^{-1}\Delta\chi(u_\lambda B_\lambda)^2$, and differentiating with respect to u_α one obtains $\partial f_M/\partial u_\alpha = -\mu_0^{-1}\Delta\chi(u_\lambda B_\lambda)B_\alpha$. It is convenient to introduce a dimensionless quantity B_α^*:

$$B_\alpha^* = \sqrt{\Delta\chi/\mu_0}\sqrt{\sigma_0^3/\epsilon_{LJ}}B_\alpha, \tag{46}$$

which leads to $\partial f/\partial u_\alpha = -(u_\lambda B_\lambda^*)B_\alpha^*$. In the following, the asterisk will be omitted. The torque due to the field exerted on particle i is then

$$\boldsymbol{T}_i^M = (\boldsymbol{u}_i\cdot\boldsymbol{B})\boldsymbol{u}_i\times\boldsymbol{B}. \tag{47}$$

V. RESULTS

A. Mięsowicz coefficients

The Mięsowicz coefficients as functions of density for $T=0.95$ and an external field $B=0.90$ are shown in Fig. 1.

As the density increases, the ratio of $\eta_3:\eta_1$ becomes smaller, with the two viscosities becoming nearly equal immediately before the nematic-smectic phase transition. The results for $N=1372$ agree reasonably well with those for $N=500$, particularly for the higher densities. The fits, for $N=500$, were performed using Eq. (44). For η_1 two fits were made, one for the regular component using data up to a density $\rho=0.20$ and one for the divergent term over the full range. The difference between the two fits becomes pronounced in the presmectic region. Only the regular term was used to fit η_2 and η_3. The fit parameters are given in Table I.

In Fig. 2, the viscosities are shown for $B=0.35$, with $T=0.95$, as above. The most obvious difference is the density at which the phase transition occurs. Again for η_1, both the regular component (using data up to $\rho=0.26$) and the divergent components were fitted, and for η_2 and η_3 only the regular part. From Table I, the critical exponent ν for $B=0.90$ is seen to correspond rather well to the helium analogy prediction of $\frac{1}{3}$. For the weaker field, $B=0.35$, ν is rather large, but the inaccuracy is such to allow $\frac{1}{3}$ (Table II). However, the result for the transition density is in agreement with that inferred from plots of structural data as a function of density. Comparing the two figures, one sees that the strength of the field has a large effect on the density at which the nematic-smectic transition occurs.

Data are available for the dependence of the Mięsowicz viscosities on temperature. However, due to the weakness of this effect at constant pressure, no results are given here.

B. Leslie and Helfrich viscosities

The dependence of the Leslie viscosities γ_1 and γ_2 on the density for $B=0.90$ is shown in Fig. 3. One sees that the relationship $|\gamma_2|>\gamma_1$ is valid throughout the nematic region, although the fits suggest that there is crossing of the viscosities for densities very close to the transition density.

There is, however, no indication that either of the two quantities diverge, as has been found experimentally and predicted theoretically. The fit parameters are given in Table III.

TABLE III. Fit parameters for the density dependence with $T=0.95$, $B=0.90$.

γ_1	$a=0.07\pm0.01$	$\epsilon=5.86\pm0.35$
$-\gamma_2$	$a=0.12\pm0.02$	$\epsilon=4.69\pm0.46$

TABLE IV. Fit parameters for the density dependence with $T=0.95$, $B=0.35$.

γ_1	$a=0.09\pm0.01$	$\epsilon=4.78\pm0.19$
$-\gamma_2$	$a=0.12\pm0.02$	$\epsilon=4.46\pm0.27$

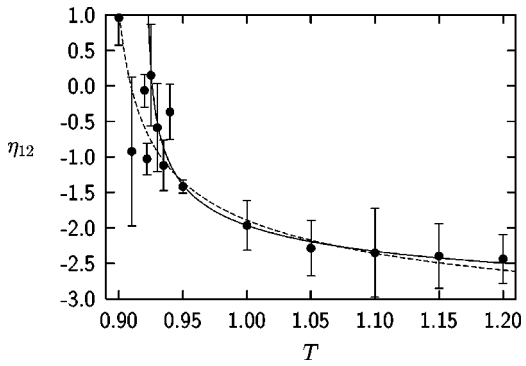

FIG. 5. η_{12} as a function of temperature with $\rho=0.275$ and $B=0.35$ for $T_{ns}=0.92$ (——) and $T_{ns}=0.89$ (− − −).

The corresponding results for $B=0.35$ can be seen in Fig. 4 (see also Table IV. Again, the absolute value of γ_2 remains larger than γ_1, although the convergence point is beyond the transition density. Here, too, the behavior of the viscosities is described better by a fit of the Arrhenius form, rather than one with a divergent term.

As can be seen in Fig. 5, the Helfrich viscosity diverges as the temperature is reduced towards the nematic-smectic transition. Since η_{12} can be of either sign, Eq. (41) was modified in an *ad hoc* manner by retaining the divergent term but replacing the Arrhenius term by a constant term, thus yielding

$$\eta_{12}(T)=b(T-T_{ns})^{-\nu}+c. \tag{48}$$

However, the parameters of the fit using Eq. (48) were subject to very large errors. Thus, the data were fitted for two specific, fixed values of T_{ns}, both of which were deemed to be plausible on the basis of the structural data. The resulting curves are shown in the figure and the ensuing parameters are given in Table V.

As one sees, the errors are rather large. However, ν seems rather insensitive to the exact position of the phase change, and for both the transition temperatures chosen, $\frac{1}{3}$ is the more likely value for ν, although $\frac{1}{4}$ cannot be ruled out, particularly since the statistics are rather poor close to the phase transition.

VI. CONCLUSIONS

For the full Gay-Berne system, one has the strength of the external orienting field B as an additional state variable. For the case $B=0.90$, similar results to those for the perfectly ordered particles are obtained. Whereas $\eta_1(\rho)$ increases rapidly with a critical exponent in good agreement with $\nu=\frac{1}{3}$, $\eta_2(\rho)$ and $\eta_3(\rho)$ display regular behavior in the presmectic region. Again, neither $\gamma_1(\rho)$ nor $\gamma_2(\rho)$ undergoes a drastic change prior to the phase transition, but here the relationship

TABLE V. Fit parameters for the temperature dependence of η_{12} with $\rho=0.275$, $B=0.35$.

T_{ns}	b	c	ν
0.89	1.14 ± 1.34	-4.28 ± 1.85	0.34 ± 0.19
0.92	0.82 ± 1.06	-3.68 ± 1.39	0.29 ± 0.20

$|\gamma_2(\rho)|>\gamma_1(\rho)$ is fulfilled. However, the difference becomes smaller as the transition is approached.

For $B=0.35$, $\eta_1(\rho)$ exhibits critical behavior at the transition, but the error is so large that both $\nu=\frac{1}{4}$ and $\nu=\frac{1}{3}$ are possible. Both $\eta_2(\rho)$ and $\eta_3(\rho)$ approximately obey an Arrhenius law, as do $\gamma_1(\rho)$ and $\gamma_2(\rho)$, with $|\gamma_2(\rho)|>\gamma_1(\rho)$. Both $\nu=\frac{1}{4}$ and $\nu=\frac{1}{3}$ are possible values of the critical exponent for $\eta_{12}(T)$.

Thus, critical exponents for the viscosities η_1 and η_{12}, and, hence for the correlation length, in broad agreement with de Gennes's helium analogy have been found. However, neither γ_1 nor γ_2 display a change of behavior at the phase transition, which is in contrast to the prediction of Jähnig and Brochard, and, for γ_1, with experimental evidence.

To explain this one may consider the relative magnitudes of the critical contributions. Using Eq. (20) to eliminate α_6 from Eq. (23), one has $\eta_1^{\rm crit}=\gamma_1^{\rm crit}$ and

$$\eta_{12}^{\rm crit}=\alpha_1^{\rm crit}=\left[\left(\frac{\xi_\parallel}{\xi_\perp}\right)^2-1\right]\eta_1^{\rm crit}, \tag{49}$$

where $\xi_\parallel$ and $\xi_\perp$ are the correlation lengths parallel and perpendicular to the director, respectively. Experimental values for $\xi_\parallel/\xi_\perp$ range from about 3 to around 6 [7]. Thus, any presmectic rise in viscosity should be strongest for η_{12}. The reason critical behavior is seen for η_1 but not for γ_1 may be connected with the fact that, whereas η_1 is determined from a single component of the pressure tensor, γ_1 is calculated from a linear combination of four components [cf. Eq. (28)] and thus subject to much greater error. While η_{12} is also obtained from a linear combination of components, the effect for this viscosity is expected to be many times larger than that for η_1 or γ_1.

Obviously no true divergence may be seen in the computer simulation, since any effect due to increasing correlation lengths is obviously limited by the finite size of the simulation box. Thus, at the nematic-smectic transition density for $T=0.95$, $B=0.90$, which is $\rho\approx0.22$, the box is roughly seven molecules long by ten molecules wide. At the higher transition densities which occur for lower external field strengths, the maximum correlation lengths are correspondingly shorter. Thus, the system may simply be too small to allow the critical behavior of γ_1 to be detected. However, it is pleasing to see that the pretransitional increase of η_1 and η_{12} could be studied so well.

[1] M. Mięsowicz, Nature (London) **158**, 261 (1946).
[2] W. Helfrich, J. Chem. Phys. **51**, 4092 (1969).
[3] S. Hess, Z. Naturforsch. A **30**, 1224 (1975).
[4] R. Schenck, Z. Phys. Chem. (Leipzig) **27**, 167 (1898).
[5] F. Hardouin, M. F. Achard, G. Sigaud, and H. Gasparoux, Phys. Lett. **49A**, 25 (1974).

[6] L. Léger and A. Martinet, J. Phys. (Paris), Colloq. **37**, C3-89 (1976).
[7] D. Langevin, J. Phys. (Paris) **37**, 901 (1976).
[8] D. D'Humières and L. Léger, J. Phys. (Paris), Colloq. **36**, C3-113 (1975).
[9] R. A. Wise, A. Olah, and J. W. Doane, J. Phys. (Paris), Colloq. **36**, C3-117 (1975).
[10] S. Bhattacharya and S. V. Letcher, Phys. Rev. Lett. **44**, 414 (1980).
[11] H. Kneppe, F. Schneider, and N. K. Sharma, Ber. Bunsenges. Phys. Chem. **85**, 784 (1981).
[12] H.-H. Graf, H. Kneppe, and F. Schneider, Mol. Phys. **77**, 521 (1992).
[13] D. Baalss and S. Hess, Phys. Rev. Lett. **57**, 86 (1986).
[14] S. Sarman and D. J. Evans, J. Chem. Phys. **99**, 9021 (1993).
[15] S. Hess, M. Kröger, W. Loose, C. Pereira Borgmeyer, R. Schramek, H. Voigt, and T. Weider, in *Monte Carlo and Molecular Dynamics of Condensed Matter Systems*, edited by K. Binder and G. Ciccotti (IPS, Bologna, 1996), Vol. 49, pp. 825–842.
[16] A. M. Smondyrev, G. B. Loriot, and R. A. Pelcovits, Phys. Rev. Lett. **75**, 2340 (1995).
[17] S. Hess, C. Aust, L. Bennett, M. Kröger, C. Pereira Borgmeyer, and T. Weider, Physica A **240**, 126 (1997).
[18] S. Cozzini, L. F. Rull, G. Ciccotti, and G. V. Paolini, Physica A **240**, 173 (1997).
[19] D. Baalss and S. Hess, Z. Naturforsch., A: Phys. Sci. **43**, 662 (1988).
[20] H. Ehrentraut and S. Hess, Phys. Rev. E **51**, 2203 (1995).
[21] G. Vertogen and W. H. de Jeu, *Thermotropic Liquid Crystals, Fundamentals* (Springer, Berlin, 1988).
[22] R. I. Tanner, *Engineering Rheology* (Clarendon, Oxford, 1988).
[23] J. J. Binney, N. Dowrick, A. Fisher, and M. E. J. Newman, *The Theory of Critical Phenomena* (Clarendon, Oxford, 1992).
[24] P. G. de Gennes, Solid State Commun. **10**, 753 (1972).
[25] F. Jähnig and F. Brochard, J. Phys. (Paris) **35**, 301 (1974).
[26] J. G. Gay and B. J. Berne, J. Chem. Phys. **74**, 3316 (1981).
[27] E. de Miguel, L. F. Rull, M. K. Chalam, and K. E. Gubbins, Mol. Phys. **74**, 405 (1991).
[28] M. P. Allen and D. J. Tildesley, *Computer Simulation of Liquids* (Clarendon, Oxford, 1989).
[29] A. W. Lees and S. F. Edwards, J. Phys. C **5**, 1921 (1972).
[30] W. G. Hoover, *Molecular Dynamics* (Springer, Berlin, 1986).
[31] S. Sarman, J. Chem. Phys. **101**, 480 (1994).
[32] A. Eich, B. A. Wolf, L. Bennett, and S. Hess, *28. Freiburger Arbeitstagung Flüssigkristalle* (Arbeitsgemeinschaft Flüssigkristalle, Freiburg i. Br., 1999).
[33] S. Hess, Z. Naturforsch. Teil A **39**, 22 (1983).